

# An Alkaline-Developable, Negative-Working Photosensitive Polybenzoxazole Based on Poly(*o*-hydroxyamide), a Vinyl Sulfone-Type Cross-Linker, and a Novel Photobase Generator

Katsuhisa Mizoguchi, Tomoya Higashihara, and Mitsuru Ueda\*

Department of Organic and Polymeric Materials, Graduate School of Science and Engineering,  
Tokyo Institute of Technology, 2-12-1 H120 O-okayama, Meguro-ku, Tokyo 152-8552, Japan

Received February 4, 2009; Revised Manuscript Received April 2, 2009

**ABSTRACT:** An alkaline-developable, negative-working, photosensitive polybenzoxazole (PSPBO) based on poly(*o*-hydroxyamide) (PHA), a cross-linker 1,6-bis(vinyl sulfone)hexane (HBVS) having a flexible aliphatic chain, and *N*-{[(4,5-methylenedioxy-2- $\alpha$ -methylnitrobenzyl)oxy]carbonyl}-2,6-dimethylpiperidine (MNCDP) as a novel photobase generator (PBG) has been developed to avoid the corrosion of copper (Cu) circuits in microchips by photogenerated acid from photoacid generators (PAGs). The resist consisting of PHA (75 wt %), HBVS (10 wt %), and MNCDP (15 wt %) showed excellent sensitivity ( $D_{0.5}$ ) of 62 mJ/cm<sup>2</sup> and a high contrast ( $\gamma_{0.5}$ ) of 4.1 when it was exposed to 365 nm wavelength light (*i*-line), postexposure baked (PEB) at 170 °C for 2 min, and developed with tetramethylammonium hydroxide aqueous solution (TMAH(aq)) at 25 °C. A fine negative pattern having 8  $\mu$ m resolution on the 2.1  $\mu$ m-thick film was obtained by exposure to 150 mJ/cm<sup>2</sup> of *i*-line by using a contact-printed mode. The resulting polymer film cured at 350 °C in an air atmosphere had a low dielectric constant ( $\epsilon$ : 2.78), high thermal stability, good mechanical properties, and low water absorption, all of which properties were comparable to those of PBO film. This novel patterning system with both a new PBG and cross-linker can be one of the candidates for the next generation microchips fabrication process which avoids corrosion of Cu circuits in semiconductor devices.

## Introduction

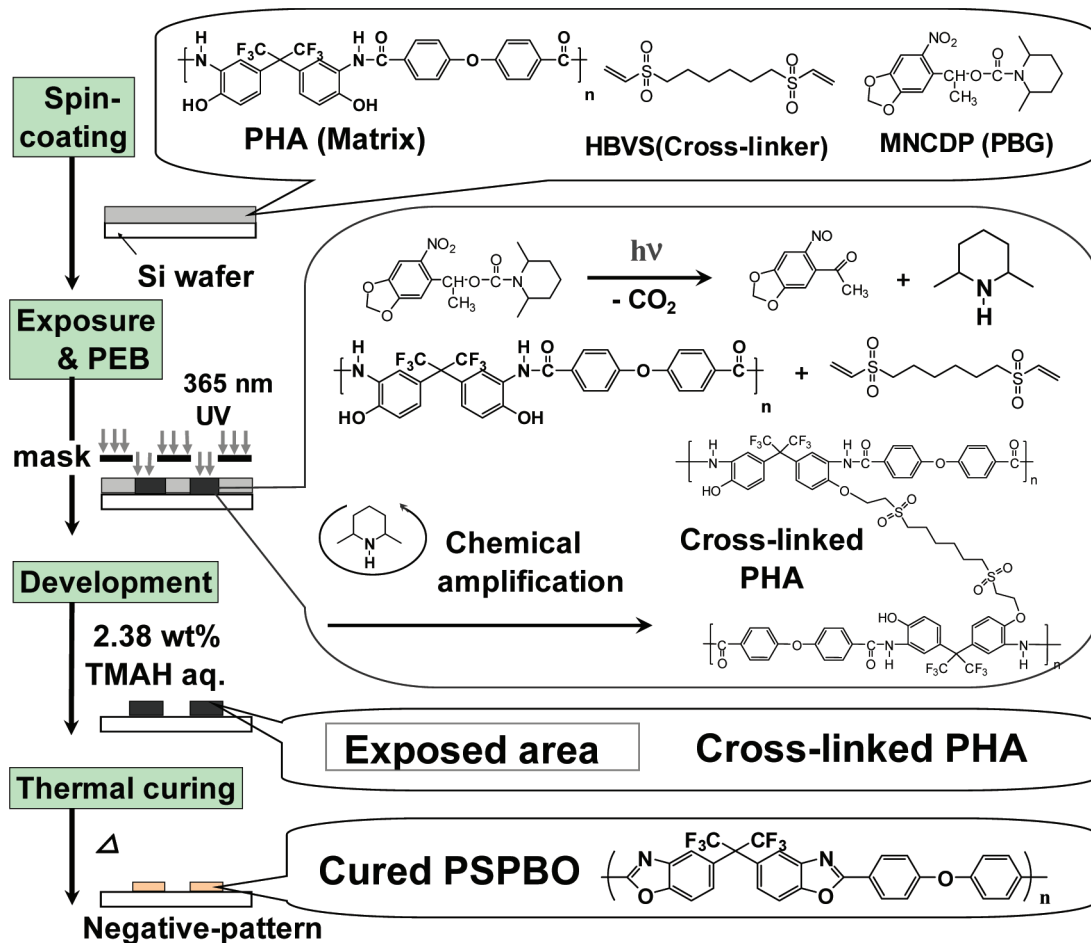
Polybenzoxazoles (PBOs) have been attracting great attention as insulating materials in the semiconductor industry due to their excellent thermal stability, high mechanical properties, and relatively low dielectric constants.<sup>1–3</sup> Additionally, the introduction of photosensitivity onto adequately alkaline-soluble PHAs as precursors of PBOs enables direct patterning with simplification of multipatterning processes.<sup>4</sup> Thereby, PSPBOs can minimize the required facilities and realize highly efficient productivity and low cost in the microelectronic manufacture. Another outstanding advantage of PSPBOs using PHAs is developability with an aqueous alkaline solution, which is environmentally friendly. Generally, PSPBOs are based on PHA with 20–30 wt % *o*-diazonaphthoquinones (DNQs), which are converted into alkaline-developable indene carboxylic acid as dissolution promoters after irradiation to give a positive pattern. However, a PSPBO resist system using DNQ requires high exposure doses in the range of 200–400 mJ/cm<sup>2</sup> to obtain a clear patterned film.<sup>5–9</sup> To improve the photosensitivity, chemical amplification by photoacid generators (PAGs), which generates sulfonic acid derivatives as catalysts, was employed by using cross-linkers or dissolution inhibitors.<sup>4,10–13</sup> On the other hand, the Cu circuits and bonding wires in recent high-speed-processing microchip devices have become narrower and narrower. Hence, there is concern that the acid derivatives from PAGs<sup>14–17</sup> and DNQs will induce the corrosion of Cu circuits and wires in next generation microchips. To remedy this problem, one of the approaches is the use of PBGs such as *o*-nitrobenzyl-derived carbamates<sup>18</sup> because there is no corrosion by organic bases. *N*-{[(4,5-Dimethoxy-2-nitrobenzyl)oxy]carbonyl}-2,6-dimethylpiperidine (DNCDP), which generates a base catalyst, 2,6-dimethylpiperidine (DMP), by *o*-nitrobenzyl photorearrangement after *i*-line exposure, has been used as a PBG for photosensitive polyimide (PSPI) resists.<sup>19–21</sup>

In a preceding paper, we reported an alkaline-developable, negative-type PSPBO based on PHA, an active ester-type cross-linker, bis(*p*-nitrophenyl)suberoylate (BNPS), and DNCDP which provides a chemically amplified PSPBO resist system without corrosion of Cu circuits.<sup>22</sup> *p*-Nitrophenol from BNPS after esterification, however, is not favorable in the process because of its volatilization and deep coloration of resists. Furthermore, DNCDP requires high irradiation doses for fine patterning formation because of the low quantum yield of DNCDP.<sup>23</sup> To overcome these problems, a new photopatterning process and a new PBG should be developed.

Here, we report an alkaline-developable and chemically amplified PSPBO resist based on PHA, HBVS as a vinyl sulfone-type cross-linker, and a new PBG, MNCDP, which provides a patterning process to avoid corrosion of Cu circuits in next generation microchips. The base-catalyzed Michael addition reaction<sup>24</sup> of vinyl sulfone units with phenolic hydroxy groups of PHA does not produce any leaving groups, and the introduction of an  $\alpha$ -methyl group in the methylene unit of the benzyl group of DNCDP may promote its hydrogen abstraction after irradiation for an effective photobase generation.<sup>25–27</sup> The photolithographic process of this PSPBO is shown in Scheme 1. The PSPBO resist varnish is spin-coated on a silicon wafer and prebaked. Then, the coated film is exposed to the *i*-line through a printed photomask to generate DMP as a base catalyst from MNCDP. Upon PEB treatment of the PSPBO film, DMP diffuses effectively and catalyzes the Michael addition reaction of the phenolic hydroxyl groups of PHA with the vinyl sulfone units of HBVS to form the cross-linked PHA. The dissolution rate of the exposed area to 2.38 wt % TMAH(aq) decreases, and a negative image is formed. Finally, the patterned PHA film is transformed into PBO film by thermal treatment. Furthermore, the thermal and mechanical properties, water absorption, and dielectric constant of the resulting PBO film are also reported.

\* To whom correspondence should be addressed: Tel +81-3-57342127; Fax +81-3-57342127; e-mail ueda.m.ad@m.titech.ac.jp.

Scheme 1. A Novel, Negative-Type PSPBO Resist System Obtained by Using a New PBG and a Vinyl Sulfone-Type Cross-Linker



## Experimental Section

**Materials.** The PHA was synthesized from 4,4'-(hexafluoroisopropylidene)-bis(*o*-aminophenol) (6FAP) and 4,4'-oxybis(benzoyl chloride) in the presence of anhydrous lithium chloride in dehydrated *N*-methyl-2-pyrrolidinone (NMP), as described previously.<sup>28</sup> The number- and weight-average molecular weights ( $M_n$  and  $M_w$ ) of PHA were 9900 and 18 900, respectively. A new PBG, MNCDP, and a vinyl sulfone-type cross-linker, HBVS, were prepared according to the procedure below. DNCDP was prepared according to the literature.<sup>19</sup> NMP, cyclopentanone, dichloromethane, and triethylamine (TEA) were distilled under reduced pressure after stirring over calcium hydride and then stored over 4A molecular sieves. 6FAP, 4,4'-oxybis(benzoic acid), polystyrene [(PS):  $M_w$  = 280 000, glass transition temperature ( $T_g$ ): 100 °C], lithium chloride, 4,5-(methylenedioxy)-2-nitrobenzaldehyde (MNA), *p*-nitrophenyl chloroformate, trimethylaluminum hexane solution [ $\text{Al}(\text{CH}_3)_3$ : 1.07 mol/L], DMP, 1-hydroxybenzotriazole monohydrate (HOBt), ethanol (EtOH), dehydrated dichloromethane ( $\text{CH}_2\text{Cl}_2$ ), 1,6-dibromohexane, 2-mercaptoethanol, potassium hydroxide (KOH: 85%), sodium hydroxide (NaOH), hydrogen peroxide ( $\text{H}_2\text{O}_2$ : 30%), methanesulfonyl chloride (MsCl), *p*-methoxyphenol (MP), phenyl vinyl sulfone (PVS), and other reagents were obtained commercially and used as received.

**Model Reaction.** To PVS (100 mg, 0.594 mmol) and MP (73.7 mg, 0.594 mmol) was added DMP (0.002 g, 0.018 mmol: 3 mol % to MP) as a base catalyst, and then the mixture was heated at 170 °C for 5 min under nitrogen in the solid state. The yield of the Michael adduct was determined by the  $^1\text{H}$  NMR spectrum in  $\text{DMSO}-d_6$  at 40 °C.

**Synthesis of 2,2'-[1,6-Hexanediyldis(thio)]bis(ethanol) (HTE).** A solution of 1,6-dibromohexane (10.0 g, 41.0 mmol) in EtOH (50 mL) was added dropwise over 15 min to a solution of KOH (85%,

6.90 g, 105 mmol) and 2-mercaptoethanol (9.61 g, 123 mmol) in EtOH (150 mL) at 2–5 °C under nitrogen, and then the reaction mixture was allowed to warm to room temperature, followed by stirring for 20 min at room temperature, and heating with stirring at 55 °C for 3 h. The solution was washed with a 5 wt % NaOH aqueous solution to remove the unconverted 2-mercaptoethanol. The resulting suspension was extracted with dichloromethane. The organic layer was washed with brine, distilled water (3 times), dried over magnesium sulfate, filtrated, and concentrated in vacuo. The white solid HTE was obtained. Yield: 3.48 g (99%); mp 44–45 °C. IR (KBr,  $\nu$ ,  $\text{cm}^{-1}$ ): 2854 and 2923 ( $-\text{CH}_3$ ,  $-\text{CH}_2-$ ), 3394  $\text{cm}^{-1}$  (OH).  $^1\text{H}$  NMR ( $\text{CDCl}_3$ ,  $\delta$ , ppm): 1.39–1.43 (m, 4H,  $\text{CH}_2$ ), 1.58–1.66 (m, 4H,  $\text{CH}_2$ ), 2.23–2.27 (t,  $J$  = 6.3 Hz, 2H, OH), 2.50–2.55 (t,  $J$  = 7.5 Hz, 4H,  $\text{CH}_2$ ), 2.71–2.75 (t,  $J$  = 6.0 Hz, 4H,  $\text{CH}_2$ ), 3.69–3.75 (q, 4H,  $\text{CH}_2$ ). Anal. Calcd for  $\text{C}_{10}\text{H}_{22}\text{O}_2\text{S}_2$ : C, 50.38; H, 9.30. Found: C, 50.09; H, 9.05.

**Synthesis of 2,2'-[1,6-Hexanediyldis(sulfonyl)]bis(ethanol) (HSE).** To HTE (4.00 g, 16.8 mmol) in acetic acid (6 mL) was added dropwise over 15 min 30%  $\text{H}_2\text{O}_2$  (3 mL) at 0 °C under nitrogen. The solution was refluxed for 3 h, and then the second portion (3 mL) of 30%  $\text{H}_2\text{O}_2$  was added.<sup>29</sup> The mixture was kept boiling until no peroxide remained, cooled, and removed under reduced pressure to yield the viscous liquid. After ca. 1 h, the liquid became a white solid. EtOH (150 mL) was added to the crude compound, and the mixture was stirred at room temperature for 1 h. Then, the filtrated solution was concentrated in vacuo to give a white solid, HSE. Yield: 2.29 g (45%); mp 94–95 °C. IR (KBr,  $\nu$ ,  $\text{cm}^{-1}$ ): 1133 and 1268, ( $-\text{SO}-$ ), 2869–2993, ( $-\text{CH}_3$ ,  $-\text{CH}_2-$ ), 3394  $\text{cm}^{-1}$  (OH).  $^1\text{H}$  NMR ( $\text{DMSO}-d_6$ ,  $\delta$ , ppm): 1.36–1.43 (m, 4H,  $\text{CH}_2$ ), 1.64–1.74 (m, 4H,  $\text{CH}_2$ ), 3.06–3.12 (t,  $J$  = 8.1 Hz, 4H,  $\text{CH}_2$ ), 3.15–3.19 (t,  $J$  = 5.7 Hz, 4H,  $\text{CH}_2$ ), 3.77–3.81 (t,  $J$  = 6.3 Hz, 4H,  $\text{CH}_2$ ), 3.79

(br, 2H, OH). Anal. Calcd for  $C_{10}H_{22}O_6S_2$ : C, 39.72; H, 7.33. Found: C, 39.45; H, 7.07.

**Synthesis of HBVS.** To a solution of HSE (1.40 g, 4.63 mmol) and  $MsCl$  (0.90 mL, 11.6 mmol) in dehydrated dioxane (50 mL) was added dropwise over 10 min a solution of TEA (6.5 mL, 46.3 mmol) in dehydrated dioxane (10 mL) at room temperature under nitrogen.<sup>30</sup> The resulting mixture was stirred at room temperature for 8 h and then was concentrated in vacuo. The residue was poured into distilled water (100 mL). The resulting solution was extracted with dichloromethane. The organic layer was washed with distilled water (2 times, 50 mL), dried over magnesium sulfate, filtrated, and concentrated in vacuo. The crude product was a white solid. The solid was recrystallized by ethyl acetate/*n*-hexane (1/4 volume ratio). Yield: 1.05 g (85%); mp 92–93 °C. IR (KBr,  $\nu$ ,  $cm^{-1}$ ): 1126 and 1288, ( $-SO-$ ), 2862–3116, ( $-CH_3$ ,  $-CH_2-$ ,  $=CH_2$ ).  $^1H$  NMR ( $CDCl_3$ ,  $\delta$ , ppm): 1.42–1.51 (m, 4H,  $CH_2$ ), 1.74–1.92 (m, 4H,  $CH_2$ ), 2.95–3.01 (t,  $J = 7.5$  Hz, 4H,  $CH_2$ ), 6.18–6.21 (d,  $J = 9.9$  Hz, 2H,  $CH$ ), 6.42–6.48 (d,  $J = 16.2$  Hz, 2H,  $CH$ ), 6.60–6.68 (q, 2H,  $CH$ ). Anal. Calcd for  $C_{10}H_{18}O_4S_2$ : C, 45.09; H, 6.81. Found: C, 44.80; H, 6.56.

**Synthesis of  $\alpha$ -Methyl-6-nitro-1,3-benzodioxole-5-methanol (MNBM).** MNA (5.00 g, 25.6 mmol) was dissolved in dehydrated  $CH_2Cl_2$  (40 mL); to the solution was added dropwise 1.07 mol/L  $Al(CH_3)_3$  hexane solution (2 equiv, 47.9 mL, 51.2 mmol) in dehydrated  $CH_2Cl_2$  (15 mL) at room temperature under nitrogen.<sup>31</sup> The mixture was stirred at room temperature for 12 h. The solution was poured into water to decompose the unconverted  $Al(CH_3)_3$ . The precipitate was removed by vacuum filtration, and the filtrated solution was extracted with dichloromethane. The organic layer was washed with brine and distilled water (3 times), dried over magnesium sulfate, filtrated, and concentrated in vacuo. The crude product was purified by flash chromatography with acetone, giving a brown solid. Yield: 4.74 g (95%); mp 79–80 °C. IR (KBr,  $\nu$ ,  $cm^{-1}$ ): 1511 and 1380, ( $NO_2$ ), 3425  $cm^{-1}$  (OH), 1033 and 1257 ( $-O-$ ).  $^1H$  NMR ( $CDCl_3$ ,  $\delta$ , ppm): 1.53–1.55 (d,  $J = 6.3$  Hz, 3H,  $CH_3$ ), 2.36 (br, 1H, OH), 5.42–5.49 (q, 1H,  $CH$ ), 6.11–6.12 (m, 2H,  $CH_2$ ), 7.27 (s, 1H, Ar), 7.46 (s, 1H, Ar). Anal. Calcd for  $C_9H_9NO_5$ : C, 51.19; H, 4.30. N, 6.63. Found: C, 51.34; H, 4.59, N, 6.43.

**Synthesis of (4,5-Methylenedioxy-2- $\alpha$ -methylnitrobenzyl)-*p*-nitrophenylcarbonate (MMN).** A solution of MNBM (3.10 g, 14.7 mmol) and *p*-nitrophenyl chloroformate (7.40 g, 36.7 mmol) in dehydrated dioxane (75 mL) was cooled in an ice–water bath. To this solution was added dropwise TEA (12.3 mL, 88.1 mmol) in dehydrated dioxane (60 mL) under nitrogen. The mixture was stirred at room temperature for 12 h.<sup>19,27</sup> Dioxane and unconverted TEA in the solution were remove under reduced pressure. The concentrated viscous solution was stirred in water. After removing water, the gum was added in isopropyl alcohol (IPA: 50 mL). The mixture was stirred at room temperature for 12 h, giving a solid. The precipitate was collected by filtration, dried in vacuo, and gave a light-brown solid. Yield 4.37 g (79%); mp 158–160 °C. IR (KBr,  $\nu$ ,  $cm^{-1}$ ): 1523 and 1349 ( $NO_2$ ), 1770  $cm^{-1}$  ( $C=O$ ).  $^1H$  NMR ( $CDCl_3$ ,  $\delta$ , ppm): 1.75–1.77 (d,  $J = 6.6$  Hz, 3H,  $CH_3$ ), 6.16 (s, 2H,  $CH_2$ ), 6.39–6.45 (q, 1H,  $CH$ ), 7.14 (s, 1H, Ar), 7.34–7.37 (d,  $J = 9.3$  Hz, 2H, Ar), 7.53 (s, 1H, Ar), 8.24–8.27 (d,  $J = 9.3$  Hz, 2H, Ar). Anal. Calcd for  $C_{16}H_{12}N_2O_9$ : C, 51.07; H, 3.21. N, 7.44. Found: C, 50.79; H, 3.38, N, 7.19.

**Synthesis of *N*-{[(4,5-Methylenedioxy-2- $\alpha$ -methylnitrobenzyl)-oxy]carbonyl}-2,6-dimethylpiperidine (MNCDP).** A solution of MMN (4.00 g, 10.6 mmol), DMP (15.0 mL, 10.0 mmol), and HOBt (1.18 g, 7.95 mmol) in dehydrated dioxane (150 mL) was stirred at 95 °C for 20 h under nitrogen.<sup>19</sup> The reaction mixture was then cooled to room temperature, and then dioxane was removed under reduced pressure. The yellow paste was stirred in a 5 wt % aqueous sodium carbonate solution (500 mL) and then distilled water (500 mL, 2 times). The paste was collected by filtration. The product was separated by chromatography (ethyl acetate/hexane = 1/2 volume ratio) as a yellow gum, which was dried in vacuo. Yield: 3.01 g (81%). IR (KBr,  $\nu$ ,  $cm^{-1}$ ): 1523 and 1349 ( $NO_2$ ), 1689  $cm^{-1}$  ( $C=O$ ).  $^1H$  NMR ( $CDCl_3$ ,  $\delta$ , ppm): 1.20–1.24 (m, 6H,  $CH_3$ ),

1.44–1.83 (m, 9H,  $CH_2$ ,  $CH_3$ ), 4.27–4.39 (m, 2H,  $CH$ ), 6.10–6.11 (m, 2H,  $CH_2$ ), 6.28–6.34 (q, 1H,  $CH$ ), 6.98 (s, 1H, Ar), 7.49 (s, 1H, Ar).  $^{13}C$  NMR ( $CDCl_3$ ,  $\delta$ , ppm): 154.9, 152.7, 147.3, 141.8, 137.4, 106.0, 105.7, 103.3, 69.45, 46.66, 30.45, 22.85, 21.34, 14.08. Anal. Calcd for  $C_{17}H_{22}N_2O_6$ : C, 58.28; H, 6.33. N, 8.00. Found: C, 58.11; H, 6.28, N, 8.02.

**Photosensitivity of PBGs.** PS (82.5 wt %) and PBG (MNCDP or DNCDP: 17.5 wt %) were dissolved in cyclopentanone. Each polymer solution (solid content: 11 wt %) was spin-casted on the quartz plate and then heated at 80 °C for 5 min. The thickness of both films was ca. 2.9  $\mu m$ . Those films were irradiated by changing exposure doses (0–20 000 mJ/cm<sup>2</sup>) of *i*-line. Besides, PS films at each exposure dose were measured by UV analysis. From the results of their UV spectra, the changes of absorbance at 345 nm of MNCDP and DNCDP, which were transformed to the estimated cleavage percentage by the following eq 1, were plotted at each exposure dose.

$$\text{estimated cleavage percentage [\%]} = \frac{[(Abs_{int}) - (Abs_{each exp})]/[(Abs_{ini}) - (Abs_{full})] \times 100 \quad (1)}$$

Three abbreviations were indicated as follows: ( $Abs_{ini}$ ) is the absorbance at 345 nm before exposure, ( $Abs_{each exp}$ ) the absorbance at 345 nm after each exposure dose, and ( $Abs_{full}$ ) the absorbance at 345 nm after an exposure dose until no change (in the case of MNCDP and DNCDP, absorbance at 345 nm after 10 000 or 20 000 mJ/cm<sup>2</sup> exposure dose, respectively).

**Dissolution Rate.** PHA, HBVS (10 wt %), and MNCDP (10, 12, and 15 wt %) were dissolved in cyclopentanone (solid content: 17 wt %). The polymer films (film thickness: 1.2–1.4  $\mu m$ ) were obtained by spin-casting from the solution on a silicon wafer. These films were prebaked at 80 °C for 10 s, exposed to 300 mJ/cm<sup>2</sup> of *i*-line, and followed by PEB at 120–170 °C for the set time. The exposed films were developed with 2.38 wt % TMAH(aq) and rinsed in water at 25 °C. The dissolution rate ( $\text{\AA}/s$ ) of the film was determined from changes in the film thickness before and after the development.

**Photosensitivity of PSPBO.** The photosensitive polymer film with 1.3  $\mu m$  thickness on a silicon wafer was prepared by dissolving PHA, a cross-linker HBVS, and MNCDP (or DNCDP) as a PBG in cyclopentanone (solid content: 17 wt %), followed by spin-casting on the silicon wafer and prebaking at 80 °C for 10 s, exposed to *i*-line irradiation with changing a dose, PEB at 170 °C for 2 min, and then developed with 2.38 wt % TMAH(aq) for 120 s at 25 °C (160 s in case of DNCDP: the developing time for 160 s is required to dissolve the unexposed area on the film). A characteristic photosensitive curve was obtained by plotting a normalized film thickness against exposure dose (unit: mJ/cm<sup>2</sup>). Image-wise exposure through a mask was carried out in a contact-printing mode.

**Water Absorption.** Water absorption (WA) was measured by immersing the film into water at 25 °C for 6 h.<sup>32</sup> After that, the film (length: 30 mm; width: 20 mm; thickness: 30–31  $\mu m$ ) was taken out, wiped with tissue paper, and quickly weighted on a microbalance. WA was estimated using the following equation

$$WA [\text{wt \%}] = (W_s - W_d)/W_d \times 100 \quad (2)$$

$W_d$  and  $W_s$  stand for the weight of film before and after immersing into water.

**Preparation of Polymer Films for TG, DMA, and Water Absorption Measurement.** A solution of PHA, HBVS, and MNCDP (75/10/15 wt %) in cyclopentanone (solid content: 35 wt %) was cast on a glass plate, prebaked at 80 °C for 30 min, exposed by *i*-line of 1000 mJ/cm<sup>2</sup>, followed by PEB at 170 °C for 5 min, cured at 200, 250, and 300 °C for each 20 min and at 350 °C for 1 h in an air atmosphere. On the other hand, a PBO film was prepared from a PHA solution, by solvent-casting on a glass plate, curing at 80, 200, 250, and 300 °C for each 20 min and at 350 °C for 1 h in an air atmosphere. The thickness of PBO and cured PSPBO films were 31 and 30  $\mu m$ , respectively.

**Measurements.** The infrared spectroscopy (IR) was taken with a Horiba FT-210 spectrophotometer. The  $^1H$  and  $^{13}C$  NMR spectra



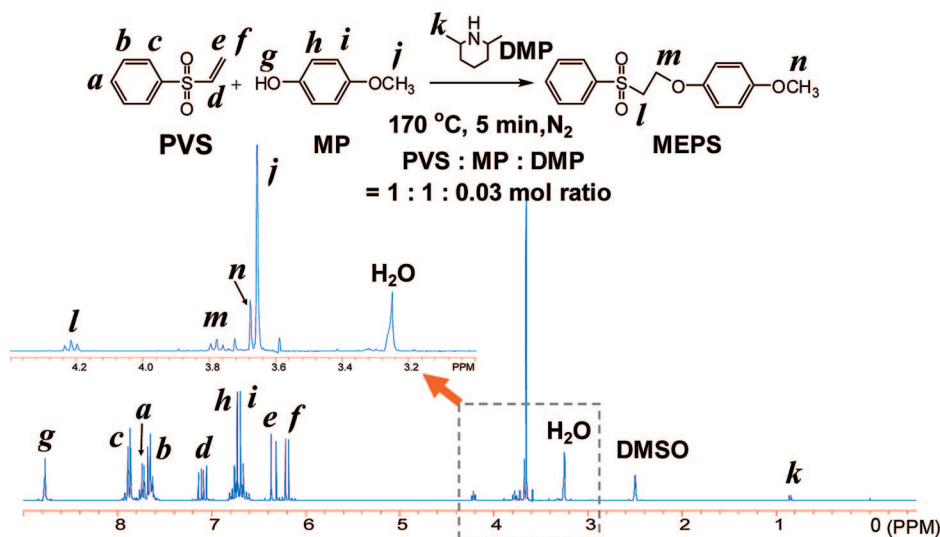


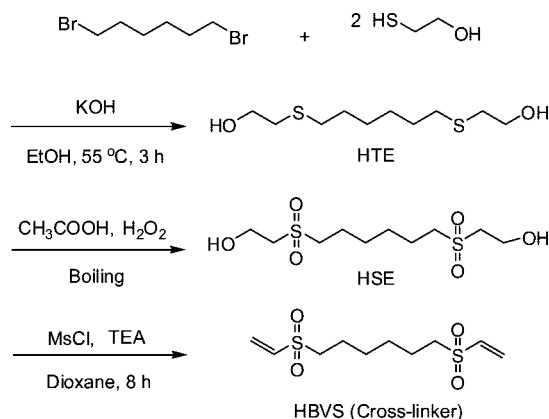
**Figure 1.**  $^1\text{H}$  NMR spectrum ( $\text{DMSO}-d_6$ ) of base-catalyzed Michael addition reaction with PVS and MP in the presence of 3 mol % DMP to MP after heating at  $170\text{ }^\circ\text{C}$  for 5 min under nitrogen.

were obtained on a Bruker DPX-300S spectrometer ( $^1\text{H}$  at 300 MHz and  $^{13}\text{C}$  at 75 MHz). Deuterated chloroform ( $\text{CDCl}_3$ ) and dimethyl sulfoxide ( $\text{DMSO}-d_6$ ) were used as solvents with tetramethylsilane as an internal standard. Elemental analyses were performed on a Yanaco MT-6 CHN CORDER with antipyrine as a standard sample. Number- and weight-average molecular weights ( $M_n$  and  $M_w$ ) were estimated by a gel permeation chromatograph (GPC) on a Jasco co-2065 Plus system equipped with a polystyrene gel column (TOSOH TSKgel GMH<sub>HR</sub>-M) eluted with THF at a flow rate of 1.0 mL/min calibrated by standard polystyrene samples. Ultraviolet–visible spectroscopy (UV–vis) was performed on a Jasco V-650 spectrophotometer. Thermal analysis was performed on a Seiko TG/DTA 6300 at a heating rate of  $10\text{ }^\circ\text{C}/\text{min}$  for thermogravimetry (TG/DTA) under the nitrogen flow rate of 200 mL/min. Dynamic mechanical thermal analyses (DMA) were performed on the PSPBO or thermally cured PSPBO films (30 mm long, 10 mm wide, and 30–31  $\mu\text{m}$  thick) on a Seiko DMS 6300 at a heating rate of  $2\text{ }^\circ\text{C}/\text{min}$  with a load frequency of 1 Hz in air.  $T_g$  is determined as the peak temperature of loss module ( $E''$ ) plots. The film thickness was measured by Veeco Instrument Dektak<sup>3</sup> surface profiler. The scanning electron microscopic image (SEM) was taken by a Technex Laboratory Tiny-SEM 1540 with 15 kV accelerating voltage for imaging. Refractive indices of PBO and the cured PSPBO resist film formed on quartz substrates were measured at a wavelength of 1320 nm at room temperature with a Metricon model PC-2000 prism coupler. Using linearly polarized laser light with parallel (TE: transverse electric) and perpendicular (TM: transverse magnetic) polarization to the film plane, the in-plane ( $n_{\text{TE}}$ ) and out-of-plane ( $n_{\text{TM}}$ ) refractive indices were measured. The dielectric constant at 1 MHz frequency was calculated from the following equation:  $n_{\text{AV}} = [(2n_{\text{TE}}^2 + n_{\text{TM}}^2)/3]^{1/2}$  and  $\epsilon = 1.10n_{\text{AV}}^2$ , where  $n_{\text{AV}}$  is an average refractive index.

## Results and Discussion

**Model Reaction for Base-Catalyzed Michael Addition.** To clarify the progress of a base-catalyzed Michael addition reaction with a vinyl sulfone compound and a phenolic derivative, a model reaction of MP with PVS in the presence of DMP as a base catalyst was carried out. A mixture of PVS, MP, and DMP (molar ratio of PVS/MP/DMP: 1/1/0.03 mole ratio) was heated at  $170\text{ }^\circ\text{C}$  for 5 min under nitrogen in the solid state. Figure 1 shows the  $^1\text{H}$  NMR spectrum of the reaction mixture. Three new peaks clearly appeared at 3.68 ppm (singlet:  $n$ ), 3.76–3.80 and 4.20–4.24 ppm (triplet:  $m$ ,  $l$ ). These peaks are assigned to methoxy and two methylene protons of the Michael adduct, 2-(4-methoxyphenoxy)ethyl phenyl sulfone (MEPS). The yield

## Scheme 2. Synthesis of HBVS

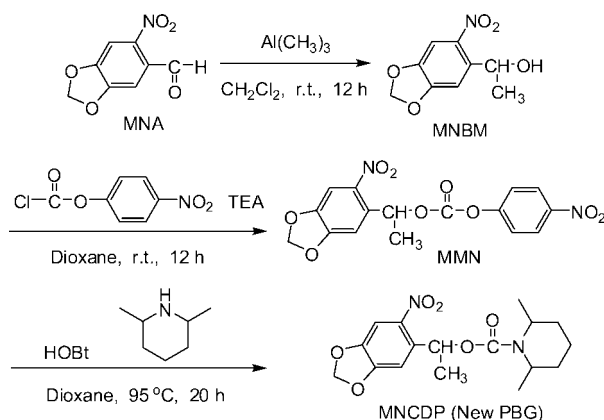


(12.8%) of MEPS was estimated by the ratio of peak areas between the methoxy protons ( $n$ ) of MEPS at 3.68 ppm and the total number of methoxy protons ( $n + j$ ) of MP and MEPS ( $j$ : 3.65 ppm) as well as the ratio of peak areas between vinyl protons ( $e + f$ ) and the aromatic protons of PVS and MEPS at 7.63–7.95 ppm.

**Synthesis of a Vinyl Sulfone-Type Cross-Linker.** In general, a cross-linking reaction is suitable to get a negative-type photosensitive polymer because a small amount of a cross-linking reaction drastically changes the solubility of a polymer. Thus, a base-catalyzed cross-linker, HBVS, having a flexible spacer for effective cross-linkage formation between polymer chains, was prepared in three steps, as shown in Scheme 2. First, HTE was prepared from 1,6-dibromohexane and 2-mercaptoethanol in the presence of KOH. Second, oxidation of HTE with  $\text{H}_2\text{O}_2$  yielded HSE. Finally, HSE was converted to HBVS by dehydration with MsCl in the presence of TEA.

**Design Consideration and Synthesis of a Novel PBG.** The *o*-nitrobenzyl group is among the well-known photochemically removable protecting ones, and the 4,5-dimethoxy-2-nitrobenzyl derivative is also known to have a low quantum yield ( $\Phi$ : 0.0013).<sup>33</sup> In general, when *o*-nitrobenzyl-derived carbamates are irradiated, the primary photochemical process is intramolecular hydrogen abstraction by the excited nitro group. This is followed by an electron redistribution process to the nitro form, which rearranges to the nitroso product, generating organic bases and carbon dioxide at the same time. In this study, to improve

## Scheme 3. Synthesis of MNCDP



the efficiency of the photobase generation of *o*-nitrobenzyl carbamate-type PBG, the introduction of an  $\alpha$ -methyl group in the benzyl unit of the methylenedioxy *o*-nitrobenzyl group was considered because intramolecular hydrogen abstraction by the excited nitro group would be promoted by stabilization of the resulting radical species. MNCDP was prepared by a three-step procedure, as shown in Scheme 3. MNA was converted to MNBM by methylation with  $\text{Al}(\text{CH}_3)_3$ , and the compound MNBM was reacted with *p*-nitrophenyl chloroformate to give MMN. Then, a reaction of MMN with DMP in the presence of HOBT yielded MNCDP. The structure of MNCDP was confirmed by FT-IR and  $^1\text{H}$  and  $^{13}\text{C}$  NMR spectroscopies. The IR spectrum of MNCDP showed characteristic absorptions at 1689, 1523, and  $1349\text{ cm}^{-1}$  due to carbamate carbonyl, nitro asymmetric, and nitro symmetric stretching vibrations, respectively. The  $^1\text{H}$  and  $^{13}\text{C}$  NMR spectra of MNCDP are presented in Figures 2 and 3 with assignments of all peaks. Furthermore, the atomic composition of MNCDP was confirmed by elemental analysis.

**Solid-State Photosensitivity of MNCDP.** The photosensitivity of MNCDP and DNCDP was investigated with thin PS films

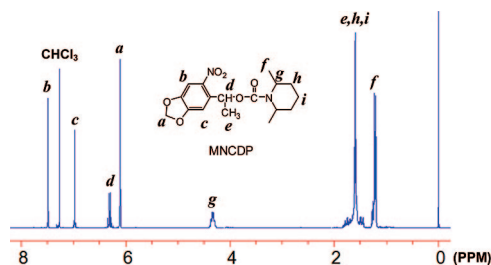


Figure 2.  $^1\text{H}$  NMR spectrum of MNCDP.

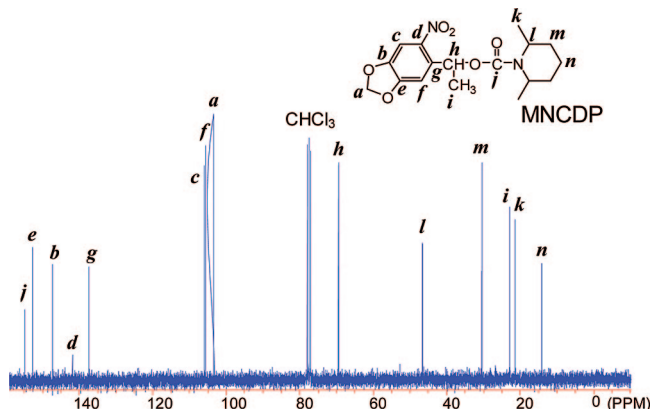


Figure 3.  $^{13}\text{C}$  NMR spectrum of MNCDP.

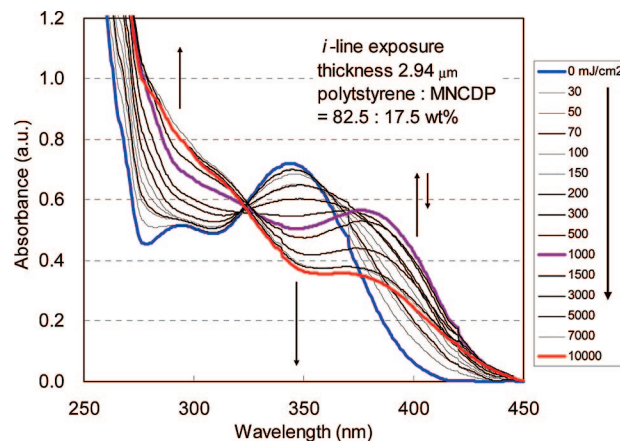


Figure 4. Change of UV-vis spectra of MNCDP in PS film on the quartz substrate under *i*-line irradiation.

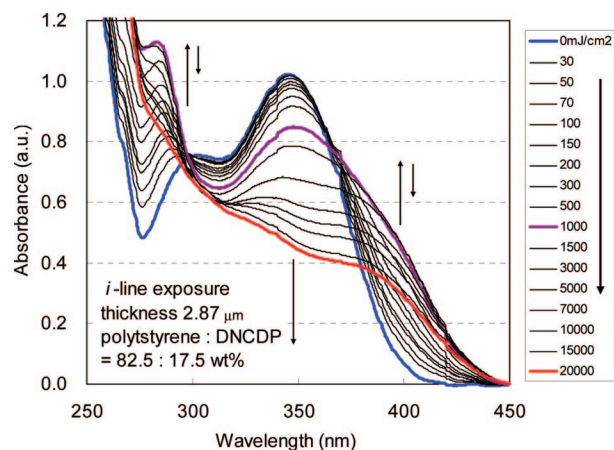
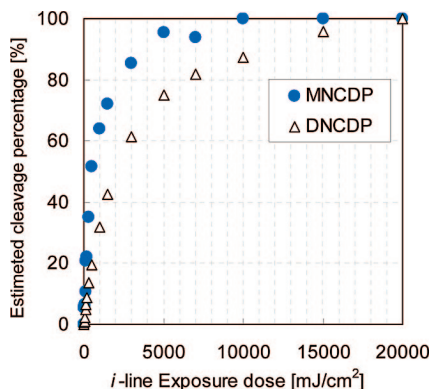


Figure 5. Change of UV-vis spectra of DNCDP in PS film on the quartz substrate under *i*-line irradiation.

containing 17.5 wt % MNCDP and DNCDP, respectively.<sup>34</sup> Figures 4 and 5 show the changes in the UV spectra of both films upon UV irradiation. PS, having the transparency at wavelength of more than 250 nm wavelength, was selected as a transparent polymer matrix for *i*-line. MNCDP shows a strong absorption centered at 345 nm, similar to that of DNCDP due to a methylenedioxy *o*-nitrobenzyl unit, and this absorbance of MNCDP at 345 nm is ca. 70% of that of DNCDP.<sup>32</sup> The absorption at 345 nm decreases slowly upon irradiation. The changes in absorbance at 345 nm, which are transformed to the estimated cleavage percentage, are plotted with each exposure dose, as shown in Figures 6 and 7. Judging from the figures, 50% cleavage of MNCDP and DNCDP require 500 and 2500  $\text{mJ}/\text{cm}^2$ , respectively. The photosensitivity of MNCDP is around 2.5 times higher than that of DNCDP at practical exposure doses of 300  $\text{mJ}/\text{cm}^2$ . The introduction of the  $\alpha$ -methyl group of the *o*-nitrobenzyl group of DNCDP accelerates its hydrogen abstraction upon *i*-line exposure compared with that of DNCDP. Therefore, MNCDP was applied for this PSPBO resist formulation.

**PSPBO Resist Formulation.** PSPBO was formulated by mixing PHA with HBVS and MNCDP, as shown in Scheme 1. HBVS is very transparent over 200 nm and does not prevent the photobase generation from MNCDP having a strong absorption centered at 345 nm.<sup>35</sup> In addition, HBVS showed good solubility in a wide range of organic solvents. Therefore, a transparent film can be obtained by spin-coating on a silicon wafer from a solution of PHA and HBVS in cyclopentanone. Besides, MNCDP and HBVS require high thermal stability



**Figure 6.** Estimated cleavage percentage of MNCDP and DNCDP in the range of 0–20 000 mJ/cm<sup>2</sup> of *i*-line.

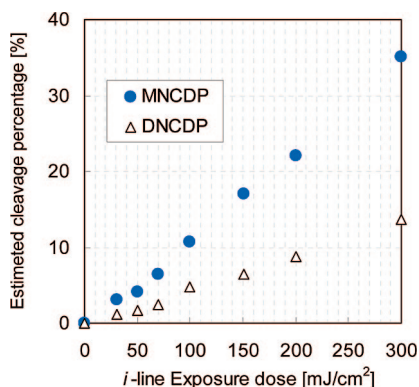


**Figure 7.** Estimated cleavage percentage of MNCDP and DNCDP in the range of 0–300 mJ/cm<sup>2</sup> of *i*-line.

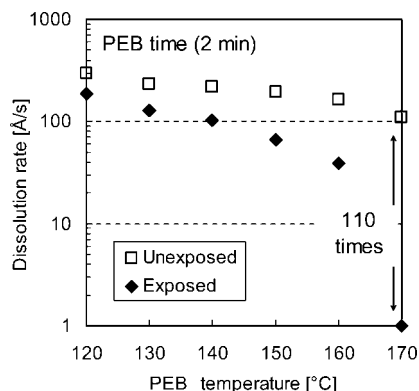


**Figure 8.** Effect of PEB temperature on the dissolution rate for the PSPBO films in the exposed and unexposed areas.

during PEB treatment. Thus, the thermal stability of these compounds was evaluated by TG analysis. The 5 wt % weight loss temperatures of MNCDP and HBVS were at 201 and 249 °C, respectively, under nitrogen, indicating their adequate thermal stability.

**Lithographic Evaluation.** To clarify the dissolution behavior of the exposed and unexposed areas toward 2.38 wt % TMAH(aq), the effects of PEB temperature and time and MNCDP loading were investigated. The 1.2–1.4  $\mu\text{m}$  thick PSPBO films were obtained by spin-coating the solution of PHA, HBVS, and MNCDP on a silicon wafer, followed by prebaking at 80 °C for 10 s in an air atmosphere, exposing to them the *i*-line of 300 mJ/cm<sup>2</sup>, and PEB at a set temperature for a prescribed period of time, and developing them with 2.38 wt % TMAH(aq) at 25 °C. The dissolution rate was estimated from the change in the film thickness before and after develop-

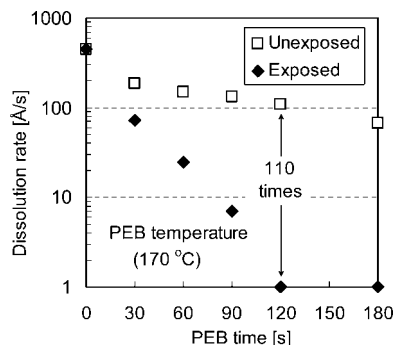


**Figure 9.** Effect of PEB time on the dissolution rate for the PSPBO films in the exposed and unexposed areas.

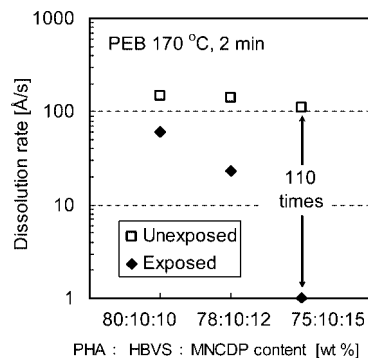


**Figure 10.** Effect of MNCDP loading on PSPBO (HBVS: 10 wt %) resist on the dissolution rate for the PSPBO films in the exposed and unexposed areas.

ment. PSPBO films composed of 75 wt % PHA, 10 wt % HBVS, and 15 wt % MNCDP were formulated. Actually, the PEB temperature in the chemical amplification system is the critical key factor for the effective diffusion of the base catalyst from PBG after irradiation and also for an acceleration of the cross-linking reaction. At first, the effect of the PEB temperature was studied, and the result is shown in Figure 8. A large dissolution contrast (DC) between the exposed and unexposed areas was obtained at 170 °C, probably because of the high diffusion of the photogenerated DMP. Next, the effect of PEB time at 170 °C was examined, as shown in Figure 9. PEB time of 2 min was sufficient to obtain a high DC. Here, it is clear that the most effective PEB condition was 170 °C for 2 min. Finally, the effect of MNCDP loading was investigated with 10 wt % HBVS loading at 170 °C for 2 min (Figure 10). The dissolution rate in the exposed area decreased by increasing MNCDP loading and the DC reached 110-fold in the presence of 15 wt % MNCDP.

On the basis of these preliminary optimizations, the PSPBO system consisting of PHA (75 wt %), HBVS (10 wt %), and MNCDP (15 wt %) was formulated. Figure 11 shows a photosensitivity curve of the optimized conditions. This resist has excellent sensitivity ( $D_{0.5}$ ) of 62 mJ/cm<sup>2</sup> and a high contrast ( $\gamma_{0.5}$ ) of 4.1 with the *i*-line. These findings indicate that the Michael addition reaction of the phenolic hydroxyl groups of PHA with HBVS catalyzed by the photogenerated base from PBG is a suitable reaction for a negative-tone image formation without an elimination component, which means that this process is environmentally friendly. The photosensitivity of the PSPBO using DNCDP was also evaluated, and the results are shown in Figure 12. This resist system exhibits lower photosensitivity of 93 mJ/cm<sup>2</sup> than the PSPBO using MNCDP, which reflects higher photosensitivity of MNCDP than that of DNCDP.

**Image Formation.** Figure 13 shows a SEM image of the line-and-space patterning of 2.1  $\mu\text{m}$  thick film obtained by a



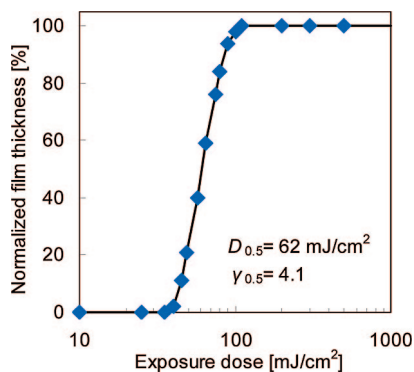


**Figure 11.** Characteristic photosensitive curve of the PSPBO resist system (PHA/HBVS/MNCDP: 75/10/15 wt %).  $D_{0.5}$  is the sensitivity, and  $\gamma_{0.5}$  is the contrast.

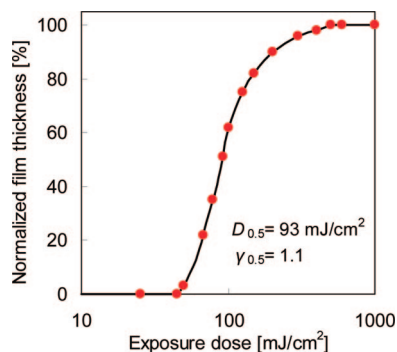


**Figure 12.** Characteristic photosensitive curve of the PSPBO (PHA/HBVS/DNCDP: 75/10/15 wt %) resist system.  $D_{0.5}$  is the sensitivity, and  $\gamma_{0.5}$  is the contrast.

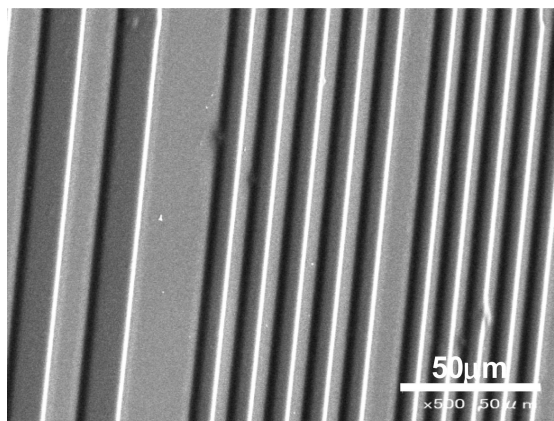


**Figure 13.** SEM image of the negative-patterned 2.1  $\mu\text{m}$  PSPBO thick film (PHA/HBVS/MNCDP: 75/10/15 wt %). The lithographic condition was as follows: 22.2 wt % solid content solution in cyclopentanone was spin-coated, prebaked at 80  $^{\circ}\text{C}$  for 10 s, exposed to 150  $\text{mJ}/\text{cm}^2$  of *i*-line, PEB at 170  $^{\circ}\text{C}$  for 2 min, developed with 2.38 wt % TMAH(aq) for 120 s at 25  $^{\circ}\text{C}$  (film thickness before and after development: 2.1  $\mu\text{m}$ ).

contact-printing mode. The clear negative-type pattern film with 8  $\mu\text{m}$  resolution is observed. This negative-patterned film is successfully converted to the PBO pattern by curing at 350  $^{\circ}\text{C}$  for 10 min in the air as shown in Figure 14. After thermal curing, the thickness (2.1  $\mu\text{m}$ ) of cross-linked PHA film was reduced to 1.6  $\mu\text{m}$  due to cyclization involving the elimination of  $\text{H}_2\text{O}$ , removal of residual solvent, the decomposition of unconverted additives such as HBVS and MNCDP, and cross-linking sites. PBO transformation was confirmed by FT-IR spectra, in which the characteristic amide carbonyl groups at 1650  $\text{cm}^{-1}$  and

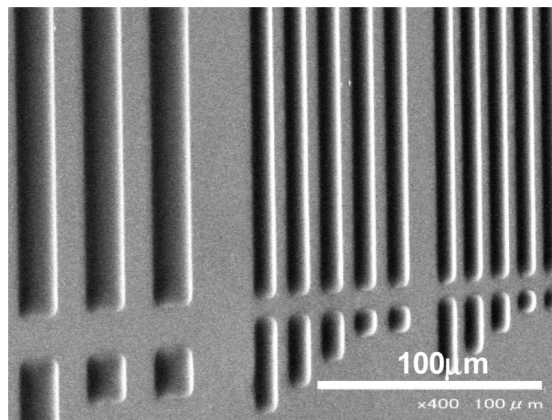


**Figure 14.** SEM image of the negative-patterned PSPBO film by thermal curing at 350  $^{\circ}\text{C}$  for 10 min (film thickness: 1.6  $\mu\text{m}$ ).

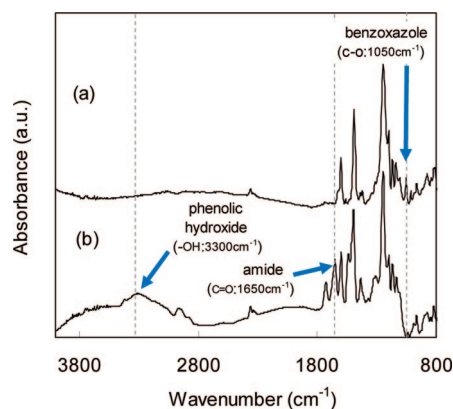


**Figure 15.** FT-IR spectra of polymer films (PHA/HBVS/MNCDP: 75/10/15 wt %) on silicon wafers. (a) The fully cured PSPBO film, prebaked at 80  $^{\circ}\text{C}$  for 10 s, exposed to *i*-line of 150  $\text{mJ}/\text{cm}^2$ , PEB at 170  $^{\circ}\text{C}$  for 2 min, cured at 350  $^{\circ}\text{C}$  for 10 min. (b) The PSPBO resist film after prebaking at 80  $^{\circ}\text{C}$  for 30 s.

**Table 1. Thermal Properties and Water Absorption of PBO and Cured PSPBO Films**

polymer films	thickness ( $\mu\text{m}$ )	$T_g^a$ ( $^{\circ}\text{C}$ )	$T_{d5\%}^b$ ( $^{\circ}\text{C}$ )	$T_{d10\%}^c$ ( $^{\circ}\text{C}$ )	char <sup>d</sup> (wt %)	WA <sup>e</sup> (wt %)
PBO	31	338	502	537	85.5	<0.05
cured PSPBO	30	not detected	495	536	85.7	<0.05

<sup>a</sup> Measured by  $E''$  of DMA. <sup>b</sup> Measured by TG. <sup>c</sup> Measured by TG. <sup>d</sup> Measured at 550  $^{\circ}\text{C}$  by TG. <sup>e</sup> Water absorption.

phenolic hydroxyl groups at 3300  $\text{cm}^{-1}$  disappear and benzoxazole absorption appears at 1050  $\text{cm}^{-1}$ , as shown in Figure 15.<sup>36</sup>

**Thermal Stability and Mechanical Properties.** The thermal properties of PBO and cured PSPBO films are summarized in Table 1. The 10 wt % weight-loss temperatures of PBO and cured PSPBO are 537 and 536  $^{\circ}\text{C}$ , respectively. The  $T_g$  of PBO is 338  $^{\circ}\text{C}$ , determined by DMA. On the other hand, no  $T_g$  of the cured PSPBO is observed probably because of cross-linking bonds.

The mechanical properties of films are crucial factors for insulating materials. Figure 16 exhibits the DMA curves of PBO and cured PSPBO films. The initial storage moduli ( $E'$ ) of PBO and cured PSPBO at 50  $^{\circ}\text{C}$  are 2.2 and 3.7 GPa, and their loss moduli ( $E''$ ) at the same temperature are 110 and 209 MPa, respectively. Thus, cured PSPBO shows higher moduli compared with PBO. Moreover, both  $E'$  and  $E''$  of cured PSPBO do not decrease up to 400  $^{\circ}\text{C}$ , which suggests that the cross-linkages between the polymer main chains slightly remain despite high thermal curing at 350  $^{\circ}\text{C}$ .

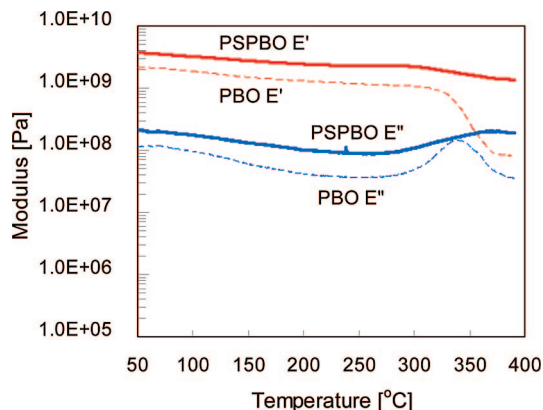


**Figure 16.** DMA curves (storage modulus  $E'$  and loss modulus  $E''$ , 1 Hz, 2 °C/min, in an air atmosphere) of PBO and cured PSPBO films.

**Table 2. Refractive Indices and Dielectric Constants of PBO and Cured PSPBO Films**

polymer films	$d$ ( $\mu\text{m}$ ) <sup>a</sup>	$n_{\text{TE}}$ <sup>b</sup>	$n_{\text{TM}}$ <sup>c</sup>	$n_{\text{AV}}$ <sup>d</sup>	$\epsilon^e$
PBO	4.3	1.5869	1.5786	1.5841	2.76
cured PSPBO	3.7	1.5918	1.5831	1.5889	2.78

<sup>a</sup> Film thickness. <sup>b</sup> In-plane refractive indices. <sup>c</sup> Out-of-plane refractive indices. <sup>d</sup> Average refractive indices;  $n_{\text{AV}} = [(2n_{\text{TE}}^2 + n_{\text{TM}}^2)/3]^{1/2}$ . <sup>e</sup> Optically estimated dielectric constant;  $\epsilon = 1.10n_{\text{AV}}^2$ .

**Water Absorption.** One of the characteristics of PBOs is low water absorption that maintains a low dielectric constant because of containing no carbonyl groups after thermal curing of PHA.<sup>4,37</sup> The water absorption of PBO and cured PSPBO films at 350 °C are summarized in Table 1. Cured PSPBO films show low water absorption (less than 0.05%), the same as the PBO film.

**Refractive Index and Dielectric Constant.** The  $\epsilon$  of the polymer films at 1 MHz can be estimated from the refractive index ( $n_{\text{AV}}$ ) of the film according to a modified version of Maxwell's equation,  $\epsilon = 1.10n_{\text{AV}}^2$ . The films of polymers on quartz plates were obtained by spin-coating from their cyclopentanone solutions, and then these films were prebaked at 80 °C for 3 min in an air atmosphere. Table 2 summarizes the refractive indices and the optically estimated dielectric constant of fully cured PBO film by thermal curing up to 350 °C for 30 min in the air, and the PSPBO resist film exposed to 150 mJ/cm<sup>2</sup>, PEB at 170 °C for 5 min, cured at 350 °C for 30 min in an air atmosphere. The average refractive indices ( $n_{\text{AV}}$ ) of the PBO and cured PSPBO films are calculated as 1.5841 and 1.5889, which are translated to  $\epsilon$  values as 2.76 and 2.78, respectively.<sup>4,10</sup> The  $\epsilon$  of both samples is almost same, which suggests that most of the additives are removed by high thermal treatment.

## Conclusions

An alkaline-developable, chemically amplified, negative-tone PSPBO resist consisting of PHA, a base-catalyzed vinyl sulfone-type cross-linker HBVS, and MNCDP as a PBG has been developed. A new *o*-nitrobenzyl carbamate-type PBG, MNCDP, which showed higher photosensitivity as compared to DNCDP, was developed as well. This PSPBO resist system provides an excellent and versatile process which avoids corrosion of Cu circuits by the acids generated from PAGs in microchips. In addition, it showed excellent sensitivity ( $D_{0.5}$ ) of 62 mJ/cm<sup>2</sup> and a high contrast ( $\gamma_{0.5}$ ) of 4.1. After the optimization of photo-

lithographic processes, a fine negative-image pattern with 8  $\mu\text{m}$  line-and-space was obtained in 1.6  $\mu\text{m}$  thin PSPBO film on silicon wafer after thermal curing at 350 °C. Also, the resulting polymer film showed a low dielectric constant and excellent thermal stability. Therefore, this PSPBO resist system can satisfy the demands for next generation microchips.

## References and Notes

- Rubner, R. *Adv. Mater.* **1990**, *2*, 452–457.
- Khanna, D. N.; Mueller, W. H. *Polym. Eng. Sci.* **1989**, *29*, 954–959.
- Yamaoka, T.; Nakajima, N.; Koseki, K.; Murayama, Y. *J. Polym. Sci., Part A: Polym. Chem.* **1990**, *28*, 2517–2532.
- Fukukawa, K.; Ueda, M. *Polym. J.* **2006**, *38*, 405–418.
- Ebara, K.; Shibasaki, Y.; Ueda, M. *Polymer* **2003**, *44*, 333–339.
- Ueda, M.; Ebara, K.; Shibasaki, Y. *J. Photopolym. Sci. Technol.* **2003**, *16*, 237–242.
- Fukukawa, K.; Shibasaki, Y.; Ueda, M. *Polym. J.* **2004**, *36*, 489–494.
- Ebara, K.; Shibasaki, Y.; Ueda, M. *J. Polym. Sci., Part A: Polym. Chem.* **2002**, *40*, 3399–3405.
- Koshiha, M.; Murata, M.; Harita, Y. *Polym. Eng. Sci.* **1989**, *29*, 916–919.
- Fukukawa, K.; Shibasaki, Y.; Ueda, M. *Macromolecules* **2004**, *37*, 8256–8261.
- Toyokawa, F.; Fukukawa, K.; Shibasaki, Y.; Ando, S.; Ueda, M. *J. Polym. Sci., Part A: Polym. Chem.* **2005**, *43*, 2527–2535.
- Shibasaki, Y.; Toyokawa, F.; Ando, S.; Ueda, M. *Polym. J.* **2007**, *39*, 81–89.
- Ogura, T.; Yamaguchi, K.; Shibasaki, Y.; Ueda, M. *Polym. J.* **2007**, *39*, 245–251.
- Naito, K.; Yamaoka, T.; Umemura, A. *Chem. Lett.* **1991**, *11*, 1869–1872.
- Naito, K.; Kanai, T.; Yamaoka, T. *J. Photopolym. Sci. Technol.* **1991**, *4*, 411–414.
- Shirai, M. *J. Photopolym. Sci. Technol.* **2007**, *20*, 615–620.
- Asakura, T.; Yamato, H.; Ohwa, M. *J. Photopolym. Sci. Technol.* **2000**, *13*, 223–230.
- Cameron, F. J.; Frechet, J. M. *J. Am. Chem. Soc.* **1991**, *113*, 4303–4313.
- Mochizuki, A.; Teranishi, T.; Ueda, M. *Macromolecules* **1995**, *28*, 365–369.
- Fukukawa, K.; Shibasaki, Y.; Ueda, M. *Polym. Adv. Technol.* **2006**, *17*, 131–136.
- Mizoguchi, K.; Shibasaki, Y.; Ueda, M. *J. Photopolym. Sci. Technol.* **2007**, *20*, 181–186.
- Mizoguchi, K.; Higashihara, T.; Ueda, M. *Macromolecules* **2009**, *42*, 1024–1030.
- Cameron, F. J.; Willson, G. C.; Frechet, J. M. *J. Am. Chem. Soc.* **1996**, *119*, 12925–12937.
- Wu, X.; Cooperman, S. B. *Bio. Med. Chem. Lett.* **2000**, *10*, 2387–2389.
- Martina, S.; MacDonald, A. S. *J. Org. Chem.* **1994**, *59*, 3281–3283.
- Pirring, C. M.; Lee, R. Y.; Park, K.; Springer, B. J. *J. Org. Chem.* **1999**, *64*, 5042–5047.
- Lia, L. S.; Babendured, L. J.; Sinhaa, C. S.; Olefsky, M. J.; Lerner, A. R. *Bio. Med. Chem. Lett.* **2000**, *17*, 3917–3920.
- Seino, H.; Iguchi, K.; Haba, O.; Oba, Y.; Ueda, M. *Polym. J.* **1999**, *31*, 822–827.
- Dsvies, G. W.; Hardisty, W. E.; Nevell, P. T.; Peters, H. R. *J. Chem. Soc. B* **1970**, *5*, 998–1007.
- Porcal, W.; Hernandez, P.; Boiani, M.; Aguirre, G.; Boiani, L.; Chidichimo, A.; Cazzulo, J. J.; Campillo, E. N.; Paez, A. J.; Castro, A.; Krauth-Siegel, L. R.; Davies, C.; Basombro, A. M.; Gonzalez, M.; Cerecetto, H. *J. Med. Chem.* **2007**, *50*, 6004–6015.
- Teague, J. S. *Tetrahedron Lett.* **1996**, *37*, 5751–5754.
- Mizoguchi, K.; Shibasaki, Y.; Ueda, M. *J. Polym. Sci., Part A: Polym. Chem.* **2008**, *46*, 4949–4958.
- Blanc, A.; Bochet, G. C. *Org. Lett.* **2007**, *9*, 2649–2651.
- Mizoguchi, K.; Shibasaki, Y.; Ueda, M. *Polym. J.* **2008**, *40*, 645–650.
- Blanc, A.; Bochet, G. C. *J. Org. Chem.* **2002**, *67*, 5567–5577.
- Fukukawa, K.; Shibasaki, Y.; Ueda, M. *Macromolecules* **2006**, *39*, 2100–2106.
- Hasegawa, M.; Tsujimura, Y.; Koseki, K.; Miyazaki, T. *Polym. J.* **2008**, *40*, 56–67.

MA900258J